

RESEARCH PAPER

Evlyn Márcia Leão de Moraes Novo
Cláudio Clemente de Farias Barbosa
Ramon Moraes de Freitas · Yosio Edimir Shimabukuro
John M. Melack · Waterloo Pereira Filho

Seasonal changes in chlorophyll distributions in Amazon floodplain lakes derived from MODIS images

Received: March 29, 2005 / Accepted: October 28, 2005 / Published online: August 28, 2006

Abstract To assess seasonal changes in phytoplanktonic chlorophyll distributions in Amazon floodplain lakes, a linear mixing model was applied to Moderate Resolution Imaging Spectroradiometer (MODIS) reflectance data acquired at four river stages: rising (April), high (June), decreasing (September), and low (November). The study area is located in a floodplain reach from Parintins (Amazonas) to near Almeirim (Pará). A three-end-member mixing model designed to uncouple three fractions [high suspended inorganic matter (ip), low inorganic suspended matter (w), and high chlorophyll *a* (Chl)] was tested in Lake Curuaí (1.5°S 55.43°W) based on field sampling done almost concurrently with satellite overpasses. During high water, phytoplankton patches are confined to lakes closer to terra firme under the influence of clear water inflow, whereas during the low and decreasing water stages, the patches are more evenly distributed over the floodplain.

Key words Amazon floodplain lakes · Chlorophyll distribution · Remote sensing

Introduction

Several studies of primary production of the Amazonian floodplains, based mainly on data from the central basin, suggest that phytoplankton production is a small fraction

of total primary production (summarized in Melack and Forsberg 2001). Isotopic studies (Forsberg et al. 1993), however, have shown that the amount of fish carbon derived from the different plant groups is not proportional to their relative contribution to the floodplain production and that algal productivity can be important.

The main challenge to further investigation of algal production at the scale of the Amazon basin is the size and complexity of the system subjected to oscillations of river discharge related to the annual cycle and interannual changes (Richey et al. 1989). Because the surface waters transport dissolved and particulate material that supports the biological system, variations of the river control the exchange of resources between the Amazon River and floodplain lakes (Forsberg et al. 1988; Richey et al. 1997). Moreover, inundation is also influenced by other water sources whose contribution to lakes depends on floodplain geomorphology (Mertes 1997), density of floodplain channels (Mertes et al. 1995), and the ratio of local drainage basin area to lake area (Forsberg et al. 1988; Lesack and Melack 1995).

To address the wide range of spatial and temporal variability, we present here results from field and satellite analyses. The synoptic view, medium resolution (250 m × 250 m), and relatively high frequency of cloud-free overpasses provided by Terra Moderate Resolution Imaging Spectroradiometer (MODIS) reflectance images make it possible to identify water color changes related to chlorophyll concentrations (Darecki and Stramski 2004). Recent applications of MODIS data to studies of aquatic systems include measurements of water quality in lakes (Koponen et al. 2004), suspended matter in coastal waters (Miller and McKee 2004), and chlorophyll concentration (Kwiatkowska and Fargion 2003).

Most inland waters are classified as Case 2 waters (Morel and Prieur 1977; Kirk 1994), in which phytoplankton concentration is not tightly coupled to the amount of total seston and optical properties are determined by a mixture of components, including phytoplankton, inorganic particles, colloids, and dissolved organic matter (Mobley 1994). Much of the research on Case 2 water has been focused on

E.M.L. de Moraes Novo (✉) · C.C. de Farias Barbosa ·
R.M. de Freitas · Y.E. Shimabukuro
Coordenação de Observação da Terra, Instituto Nacional de
Pesquisas Espaciais, São José dos Campos, Avenida dos
Astronautas, 1758, CEP 12 201 970, Brazil
Tel. +55-12-3945-6433; Fax +55-12-3945-6488
e-mail: evlyn@ltdid.inpe.br

J.M. Melack
Bren School of Environmental Science and Management, University
of California, Santa Barbara, CA, USA

W.P. Filho
Departamento de Geografia, Universidade Federal de Santa Maria,
Faixa de Camobi, km 9, Campus Universitário, Santa Maria, CEP
97105-900, Rio Grande do Sul, Brazil

methods for analyzing the reflectance as a function of the concentrations of phytoplankton groups, inorganic matter, and dissolved organic matter. Most of the algorithms developed for estimating chlorophyll concentration from inland aquatic systems are based on reflectance spectra derived from ground measurements and airborne sensors (Lathrop and Lillesand 1986; Dekker 1993; Novo et al. 1991) or from satellite sensors not tuned to the radiometric and spectral resolution requirements of Case 2 waters. The algorithms are generally site specific and empirically derived through statistical relationships between reflectance and chlorophyll *a* concentration. Several authors have proposed approaches to uncouple the chlorophyll signal from the remaining optical components, such as reflectance ratios (Carder et al. 1991; Tassan 1995; Arenz et al. 1996), derivative analyses (Goodin et al. 1993), neural network modeling (Keiner and Yan 1998), and principal-component analyses (Galvão et al. 2003). Pilorz and Davis (1990) suggested the use of libraries of absorption and scattering coefficients to model the upwelling reflectance for different optical water constituents. Those modeled spectra could then be applied as end-members for the application of mixing algorithms (Mertes 1990).

Novo and Shimabukuro (1994) proposed the use of mixing models to uncouple field reflectance spectra. The measured reflectance at a particular location represented the sum of the spectra of several optically active components, and each spectrum was weighted by the relative proportion of each component in the sample. They used a least square fitting approach to uncouple three end-members: high concentration of chlorophyll *a*, suspended inorganic matter, and water. In spite of the limitations of the approach, given the complexity of aquatic systems, the authors concluded that the fraction of chlorophyll reflectance accounting for the reflectance spectra of the various samples correlated significantly with chlorophyll concentration.

In the present research, intensive field data collected concurrently with satellite overpasses at a test site were used to empirically derive a model to estimate chlorophyll *a*

concentrations from chlorophyll fraction images computed from MODIS data. This model was then assessed by comparing measured and estimated chlorophyll *a* for the different dates. The final model was then applied to a MODIS monthly series to assess chlorophyll distributions from Parintins (Amazonas) to near Almeirim (Pará).

Materials and methods

Site description

The study area encompasses the Amazon floodplain from the Parintins (AMAZONAS) at 02°37'42" S 56°44'09" W to west of Almeirim (Pará) at 01°31'24" S 52°34'54" W. This floodplain is characterized by large shallow lakes (Sippel et al. 1992) with average depth ranging from 1 to 3 m over the hydrological cycle. The Amazon and the Tapajós rivers are the major sources of water to the floodplain in this reach. Lago Grande de Curuaí (Curuaí Lake) was selected as a test site for intensive water sampling concurrently with Terra MODIS overpasses.

Curuaí Lake is composed of several depressions, which at high water coalesce into Lago Grande de Curuaí (1.5° S 55.43° W). It is located along the Amazon River, 900 km upstream from the river mouth at the Atlantic Ocean (Fig. 1).

The lake receives different types of water, i.e., white water from the Amazon River during the overflow stage and black and clear water from the local catchments during the low stage (Barbosa 2005). The lake's ecology is modulated by fluctuations in Amazon River water level (Fig. 2), which are characterized by four stages: a period of rapid rise of water level from January to the end of February with rising rates more than 0.2 cm h⁻¹; a period of overflow from April to the end of June when water enters breaks in the levees with decreasing rising rates (less than 0.2 cm h⁻¹) until overtopping the levees; a period of rapid fall in water level

Fig. 1. Study area and test site location. Curuaí Lake was the test site used to calibrate the model to map the chlorophyll distribution in the study area



Fig. 2. Amazon River daily average water level fluctuation at Curuaí (C. Barbosa, unpublished data)

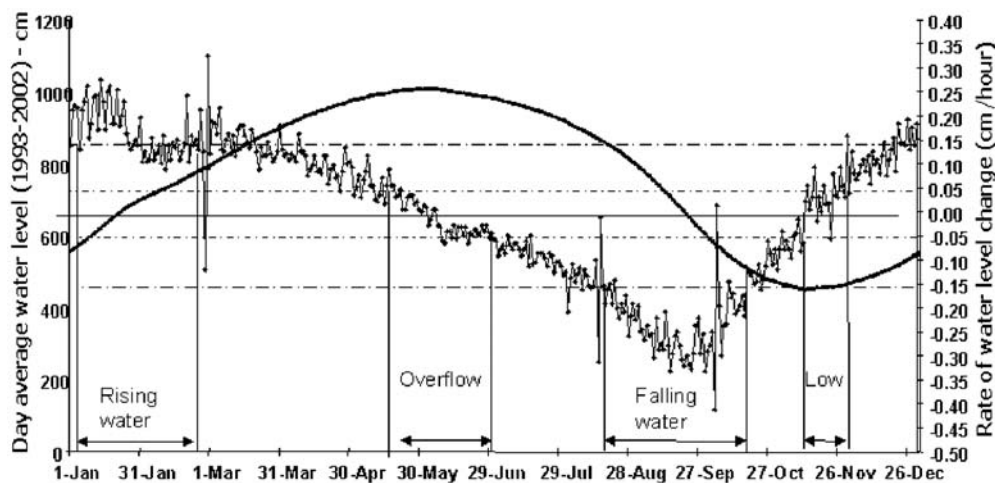


Table 1. The 95% confidence interval for the average of the mean daily chlorophyll (Chl) concentration ($\mu\text{g l}^{-1}$) for each in situ data collection at Curuaí Lake test site along the hydrological cycle

Month	95% Confidence
September 2003	51 < Chl < 76
November 2003	29 < Chl < 36
February 2004	7 < Chl < 9
June 2004	23 < Chl < 33

from August to October with falling rates more than 0.2 cm h^{-1} ; and a period of low water level from October to November.

Experimental procedure

From 2003 to 2004, field campaigns were undertaken to measure the concentrations of optically active components in Curuaí Lake. The campaigns spanned the seasonal changes in the Amazon River's hydrograph. The average time spent on each campaign was 10 days, with about seven stations sampled per day. The mean daily average concentrations of chlorophyll remained relatively constant during the period of each campaign (Table 1).

To guide sampling, MOD 09 images were downloaded from the Land Processes Distributed Active Archive Center (LP DAAC), located at the U.S. Geological Survey EROS Data Center (<http://LPDAAC.usgs.gov>), before each field campaign. The number and position of samples were defined by examining historical Landsat-TM images representative of each water stage. For each date, at least 70 sites covering the entire lake (Fig. 3) were identified for determination of the concentration of chlorophyll (Chl), suspended inorganic particles (ip), and dissolved organic carbon (DOC).

Water samples were collected from 09:00 to 15:00 at a depth midway between the surface and Secchi depth because this region contributes up to 90% of the upwelling radiation (Kirk 1994). Chlorophyll concentration determined at this depth can be regarded as a proxy of the average chlorophyll concentration in the euphotic zone in

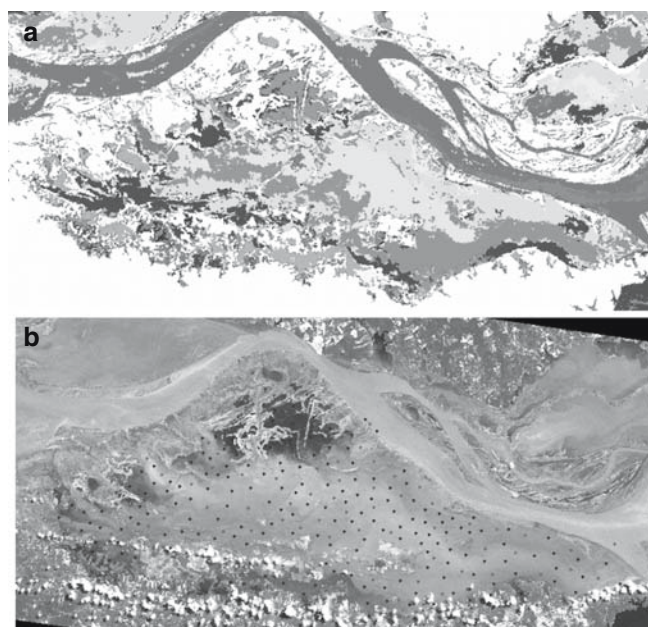


Fig. 3. **a** Spectral differences in lake water masses as shown by an unsupervised classification of TM-Landsat image acquired at high water. **b** Ground sampling distribution selected to represent the spectrally different water masses

unstratified eutrophic shallow lakes (Morel and Berthon 1989; Cestari et al. 1996).

For chlorophyll determination, water samples were filtered through Whatman GF/F filters wrapped in aluminium foil and stored frozen (-20°C) until the analysis was completed (up to 2 weeks later). Chlorophyll determination was performed according to Nush (1980). Filters were extracted with 80% ethanol at 75°C for 5 min followed by submerging the tubes in water near freezing. The extracts were kept for 6 to 24 h in the refrigerator before spectrophotometric determination. Suspended inorganic particle determination was based on Wetzel and Likens (1991). A known volume of lake water was filtered through a GF/C filter pre-ashed at 480°C and preweighed. Filters were stored in desiccators over silica gel. In the laboratory, the filter was dried at 60°C

for 24 h and weighed to determine total suspended matter. The same filter was ashed at 480°C for 1 h and reweighed to determine inorganic particle concentration. For dissolved organic carbon (DOC) determination, lake water was passed through a pre-ashed Whatman GFC filter, and the filtrate was collected in 15-ml flasks and preserved with HCl. Samples were run in a combustion/nondispersive infrared gas analyzer according to APHA (1998).

MOD 09 Level 2 G Validated Version 3 images were examined to select scenes free from cloud cover and glitter. Corrections were made for the effect of atmospheric gases, aerosols, and thin cirrus clouds (<http://lpdaac2.usgs.gov/modis/mod09ghk.asp>). MOD 09 images were first transformed from the Integerized Sinusoidal (ISIN) projection to Lat/Long projection using the MODIS Reprojection Tool (<http://lpdaac2.usgs.gov/landdaac/tools/modis/about.asp>). Images were resampled to 250 m using a nearest neighbor algorithm. The output image was saved in Geotiff format and compressed from 16 to 8 bits. The compression was done using a tool (N. Arai, personal communication) that fits the reflectance distribution in the scene to an 8-bit image, tuning the look-up table to the user-defined reflectance range. The look-up table was optimized for an aquatic environment characterized by low reflectance values.

The MODIS data set was masked using a wetland mask (Hess et al. 2003) to limit the analyses to the floodplain. A series of prospective end-member samples were selected to run a linear mixing model with the aid of field sampling of the major optical active components in the open water at four hydrograph stages. All the field information on concentration of the optically active components was used interactively to locate “pure pixels” within the dataset. The candidate “pure pixels” were plotted in all spectral bands. Sampling sites characterized by high concentration of chlorophyll and low concentration of the other active components were selected if the spectral curve displayed by the pixel matched the spectrum of chlorophyll-laden water. The same procedure was applied for each optically active component on all dates.

Figure 4 shows the examples of candidate end-members selected to decompose MODIS pixels into proportions of reflected signal for each selected components. The analysis of those end-members showed that the spectral curves of DOC-laden water (black water) and water (clear water) were similar and flat. Hence, they were grouped into what was operationally defined as a low inorganic suspended particle end-member (w) to represent the spectral contribution of a pure pixel encompassing samples with low signal coming from the water.

Linear spectral unmixing is an approach to uncouple a mixture of components in a pixel (Shimabukuro and Smith 1991). The linear mixture model can be defined as follows. Let $S(x,y)$ be the spectral signature collected by the sensor at the pixel with spatial coordinates (x,y) . This signature can be considered a n -dimensional vector, where n is the number of spectral bands; it can also be modeled as a linear combination of end-member vectors E_i , $i = 1, E$, using the following expression:

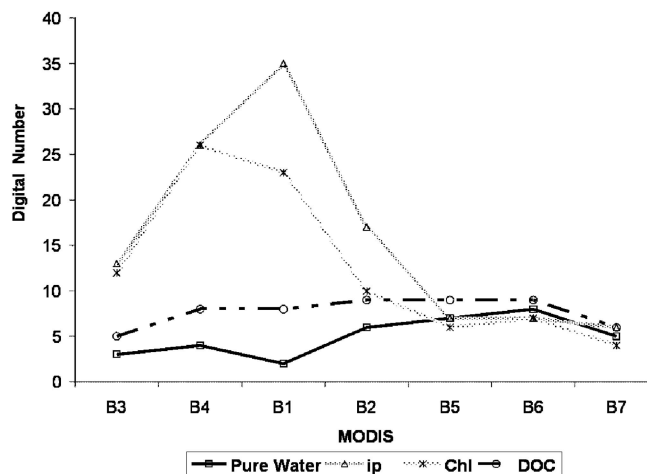


Fig. 4. Candidate end-members used to run the linear mixing model. The x-axis shows the Moderate Resolution Imaging Spectroradiometer (MODIS) bands as follows: B3, 459–479 nm; B4, 545–565 nm; B1, 620–670 nm; B2, 841–876 nm; B5, 1230–1250 nm; B6, 1628–1652 nm; B7, 2105–2155 nm. *Digital number* is proportional to the reflectance in each band

$$S(x,y) = \sum_{i=1}^E f_i(x,y) \epsilon_i$$

where $f(x,y)$ is a scalar value representing the fractional coverage of end-member vector E_i at pixel $S(x,y)$ and ϵ_i is the fitting error.

The linear mixing model with three end-members incorporated the contribution of water (w), phytoplankton (phy), and inorganic particles (ip) to the reflectance of each MODIS band as follows:

$$Bn_{ref} = f_w(Bn_w) + f_{phy}(Bn_{phy}) + f_{ip}(Bn_{ip})$$

and

$$f_w + f_{phy} + f_{ip} = 1$$

where Bn_{ref} is the digital number (DN) proportional to the reflected energy as measured by MOD 09 bands and f_w , f_{phy} , and f_{ip} are the fraction of each end-member contributing to the reflectance signal at the pixel S .

A September 2003 MODIS image was selected to derive the empirical model relating chlorophyll concentration to the f_{phy} image, i.e., the image representing the proportion of the chlorophyll signature to the overall reflectance of a given pixel. This date was selected because chlorophyll concentrations spanned most of the concentrations found on other dates (Table 2) and the image had high radiometric quality in compared to the other dates.

Correlation and regression analysis were applied to relate the phytoplankton fraction image to chlorophyll concentration measured at Curuaí Lake. Several iterations were required to obtain a suitable statistical model. The following statistical parameters were computed: r , adjusted R^2 , standard error of the estimate (SE), and Student's t test at the 95% significance level.

Table 2. Optical components descriptive statistics

	November 2003		September 2003		February 2004		June 2004	
	Chl	ip	Chl	ip	Chl	ip	Chl	ip
Average	30.7	458.6	89.2	49.0	8.2	94.6	28.1	8.8
Standard deviation	3.8	122.2	227.4	24.9	4.3	56.8	12.9	7.9
Coefficient of variation	12%	26%	255%	50%	50%	60%	46%	89%
Maximum	87.9	1007.1	1951.9	132.5	25.8	308.6	131.3	58.7
Minimum	0.8	9.0	4.2	2.3	0.2	35.9	0.7	1.5

Chl, chlorophyll *a* concentration ($\mu\text{g l}^{-1}$); ip, suspended inorganic matter concentration (mg l^{-1})

Source: C. Barbosa, unpublished data

Table 3. Correlation analysis

Data sets	Correlation coefficient (<i>r</i>)	Number of samples (<i>n</i>)	Significance level ($\alpha = 0.05$)
All data	-0.08	70	Not significant
6 Days from MODIS September overpass	0.37	66	Not significant
5 Days from MODIS September overpass	0.59	56	Significant
4 Days from MODIS September overpass	0.60	44	Significant
3 Days from MODIS September overpass	0.59	32	Not significant
2 Days from MODIS September overpass	0.57	19	Not significant
MODIS September overpass	0.06	4	Not significant
Samples acquired in October with suspended inorganic matter in the range of $52 \pm 23 \text{ mg l}^{-1}$	0.87	19	Significant
Samples acquired in October disregarding the suspended inorganic matter concentration range	0.70	25	Significant

MODIS, Moderate Resolution Imaging Spectroradiometer

Results and discussion

Statistical analysis

Table 2 summarizes the data obtained from the field measurements. September was the period with the highest coefficient of variation for chlorophyll. As the influence of inorganic particles in Amazon white water decreases in September, the light environment becomes more favorable for phytoplankton growth, and, as the water levels fall, Curuaí Lake divides into isolated basins under the influence of local conditions. These conditions are likely to lead to spatial variability in chlorophyll. In November the water level was lowest and conducive to wind-driven suspension of the sediments, hence the high concentration of inorganic particles and the relatively lower chlorophyll concentration. In February turbid Amazon water began to enter the lake, and the chlorophyll concentration declined because of reduced phytoplankton growth. In June, chlorophyll concentration

was higher than in February as inorganic particles decreased and the light environment became conducive to phytoplankton growth.

If the entire set of ground measurements is used to derive a correlation between the phytoplankton fraction (f_{phy}) and chlorophyll concentration (Chl), the correlation coefficient approaches zero (Table 3), i.e., there is no correlation between the f_{phy} derived from the MOD 09 scene acquired on September 29, 2003 and the chlorophyll measurements obtained from September 25 to October 7. However, as the time lag between the date of sampling and satellite image acquisition date decreases, the correlation between Chl and f_{phy} increases and becomes significant. The highest correlation occurred when the samples used to run the model were confined to data collected after the satellite overpass and restricted to water masses with concentrations of suspended inorganic particles (ip) in the range $52 \pm 23 \text{ mg l}^{-1}$. Those samples were then used to derive a model to predict chlorophyll concentration as a function of the f_{phy} .

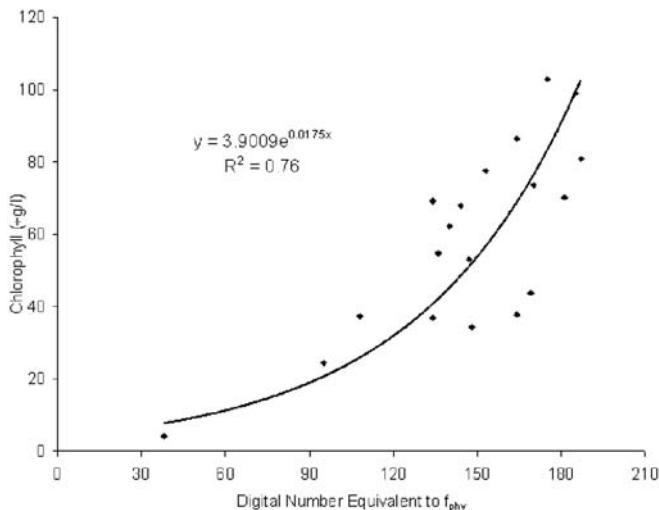


Fig. 5. Chlorophyll empirical model, where Chlorophyll ($\mu\text{g l}^{-1}$) represents the Chlorophyll a concentration and f_{phy} represents the Digital Number equivalent to the phytoplankton fraction image derived from the unmixing model.

The regression equation ($\text{Chl} = 3.9e^{0.0175f_{\text{phy}}}$) expresses a nonlinear relationship between Chl and the phytoplankton fraction image (Fig. 5). The standard error of estimate provided by the model is 19mgm^{-3} and the adjusted R^2 is 0.76; i.e., the model predicts, with an error of about 25%, chlorophyll concentration in the range between 10 and 120mgm^{-3} in areas with ip concentrations of $52 \pm 23\text{mg l}^{-1}$. This range corresponds to digital numbers (DN) equivalent to phytoplankton fraction (f_{phy}) from 40 to 180.

The field measurements have a much wider range of Chl and ip concentrations (see Table 2) than are incorporated into the regression model. To circumvent this problem, lakes subjected to high prediction errors, i.e., outside the fraction image between 40DN and 180DN, were masked and included in a single class representing concentrations outside the reliable range. Amazon River was also masked and not included in the model estimates because very few samples were collected in the river. The classes adopted to map the chlorophyll concentration were $\text{Chl} < 20\text{mgm}^{-3}$; $20\text{mgm}^{-3} < \text{Chl} < 56\text{mgm}^{-3}$; $56\text{mgm}^{-3} < \text{Chl} < 92\text{mgm}^{-3}$; $92\text{mgm}^{-3} < \text{Chl} < 110\text{mgm}^{-3}$; $\text{Chl} > 110\text{mgm}^{-3}$; and other (including cloud cover, sandbars, lake bottom, and aquatic vegetation). This strategy was adopted such that the September model could be applied to all dates. The class intervals are wide and loose enough to accommodate model uncertainty.

Empirical model validation

To validate the empirical model suitability, it was applied to the image and the estimated chlorophyll concentration was compared to measured chlorophyll concentrations at control points for different hydrological states. Figure 6 shows the results for September. It is clear that there is a good agreement between the estimated and the measured chlorophyll concentration within the defined boundary conditions,

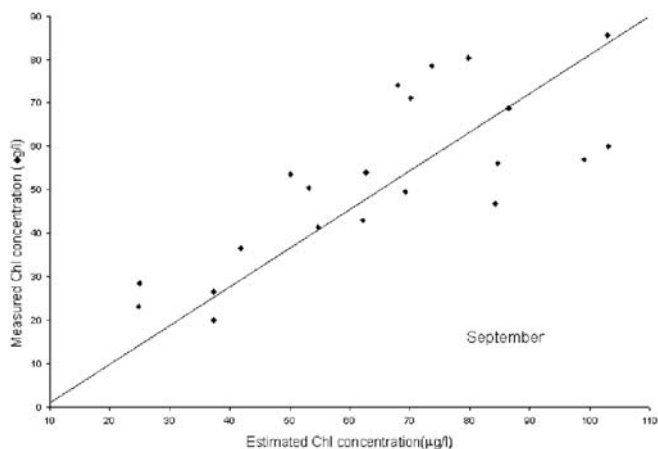


Fig. 6. Estimated versus measured chlorophyll (Chl)

which suggests that the model allows estimating the chlorophyll distribution provided that the class intervals are large enough to accommodate model variability.

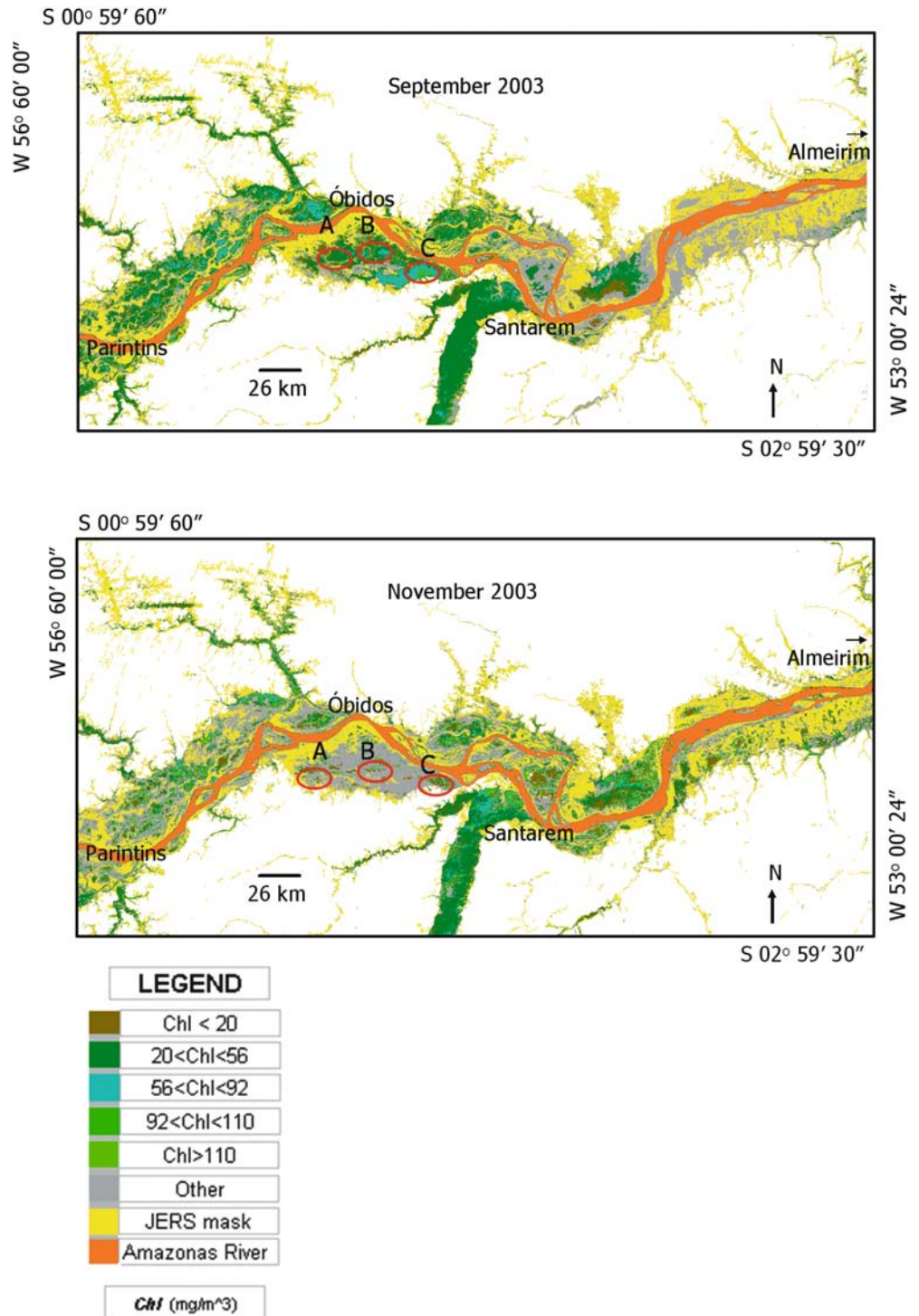
After demonstrating that the regression model was able to represent the spatial distribution of chlorophyll concentration in Curuaí Lake, the next step was to apply the model to the entire study area. As field samples were available for September 3 and November 3, the mapping was done for these two dates to assess how changes in the actual chlorophyll concentration from September to November were consistent with modeled chlorophyll (Fig. 7).

The change in phytoplankton abundance downstream of Santarém from September to November is apparent in Fig. 7. In September, the floodplain lakes upstream of Santarém (westward) have higher chlorophyll concentrations than do downstream lakes. In November, however, the pattern changes and most of the area upstream of Santarém is included in the class “Others.” Downstream of Santarém there is a decrease in the class “Others” and an increase in the classes with high concentrations of chlorophyll. The class “Others” gathers a variety of targets spanning from lake bottom newly occupied by terrestrial vegetation to cloud cover and cloud shadow. Therefore, little can be said about those changes. Several hypotheses, however, may help to explain changes in chlorophyll concentration. (1) Increased input of Tapajós River water (clear water) to floodplain lakes downstream will improve underwater light availability for phytoplankton. The Tapajós River level starts to rise in October as the rainy season begins in the Southern Hemisphere. (2) The use of the floodplain around Parintins (A.L.M. Albernaz, personal communication) for cattle increases as the water level drops and is responsible for eutrophication. Downward from the Tapajós–Amazon confluence, the herds found in the floodplain decrease.

Seasonal changes in phytoplankton

The chlorophyll maps were used to compute the weighed average of chlorophyll concentration from MODIS phy-

Fig. 7. Chlorophyll *a* distribution from Parintins to near Almeirim villages in September (top) and November (bottom) 2003. A, B, and C are locations where estimates of chlorophyll concentration have not changed over time



toplankton fraction images in the region from Parintins (Amazonas) to nearby Almeirim (Pará) for the years 2002 and 2003. The chlorophyll values were plotted against the water level (Fig. 8).

Figure 8 shows that there is an almost 6-month offset between the maximum water level in the region and the maximum average weighed chlorophyll concentration in the study area. The highest water levels were observed from April to June whereas the highest weighed chlorophyll concentration occurred in November and December for both

years, 2002 and 2003. That the pattern occurred in both years suggests that the MOD 09 chlorophyll model was successful in capturing the regional pattern of phytoplankton abundance in this floodplain reach. The data suggest that the phytoplankton peak production is achieved when the Amazon pulse recedes and the lakes are enriched by dissolved nutrients but less turbid water.

The results show that there is a time frame for high phytoplankton production that may have implications in fishery management. This study also shows a contrasting

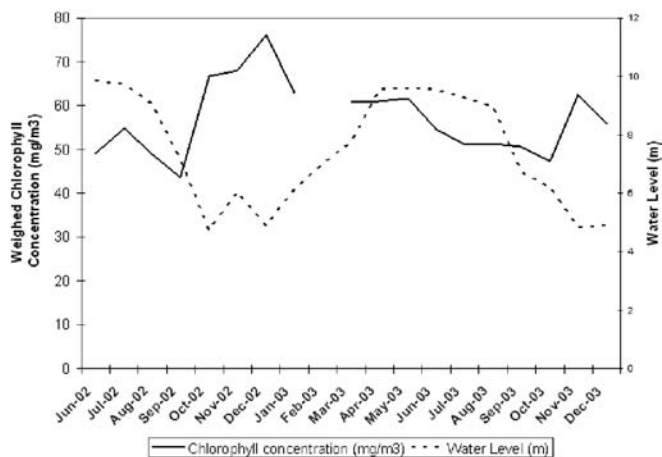


Fig. 8. Chlorophyll *a* concentrations and water level changes in the study area

pattern between the phytoplankton distribution upward and downward from the Tapajós–Amazon confluence, suggesting that the Tapajós River may play an important role in floodplain phytoplankton production during the period of low water in the Amazon River. Changes in floodplain land use may also contribute to the patterns.

According to Forsberg et al. (1993), there is a large contribution of phytoplankton to many commercial fish species, which suggests that the algal production in floodplain lakes may play an important role for the commercial fish production in the region. Studies of fisheries at Curuaí Lake (Isaac et al. 2003) show that the highest catches occur during high water because at that time large commercial boats have access to the lake. During low water, only the small boats of local fisherman are able to catch fish.

The recent soybean cultivation in Pará may represent a threat to the natural pulsations of phytoplankton production and to commercial fisheries. The grain terminal at the port of Santarém, with a capacity of up to 75 000 tons, has attracted new investors to the region, pushing ranchers and slash-and-burn farmers to new forest frontiers and into the floodplain. This intrusion may bring changes in regional scale that can only be accessed if remote sensing tools are integrated in studying the limnology of floodplain lakes.

Acknowledgments The authors thank the continuing support of FAPESP (Process. 2003/00785-3), of the Geoma Network and NASA LBA-ECO, and the LBA Office in Santarém for logistics and Gilson Rego and Flaurido Rego for assistance in the field.

References

- APHA (1998) Standard methods for the examination of water and wastewater, 20th edn. American Public Health Association, Washington, DC
- Arenz RF, Lewis WM, Saunders JF (1996) Determination of chlorophyll and dissolved organic carbon from reflectance data for Colorado reservoirs. *Int J Remote Sens* 17:1547–1566
- Barbosa CCF (2005) Sensoriamento remoto da dinâmica de circulação da água do sistema planície de Curuaí/Rio Amazonas. PhD thesis.

- National Institute for Space Research (INPE), São José dos Campos, Brazil
- Carder KL, Hawes SK, Baker KA, Smith RC, Steward RB, Mitchell BG (1991) Reflectance model for quantifying chlorophyll *a* in the presence of degradation products. *J Geophys Res* 96:20599–20611
- Cestari AC, Krug T, Novo E (1996) Modelo empírico para a estimativa da concentração da clorofila na zona eufórica em função da concentração de clorofila na superfície. *Simpósio Brasileiro de Sensoriamento Remoto* 8:93–98
- Darecki M, Stramski D (2004) An evaluation of MODIS and SeaWiFS bio-optical algorithms in the Baltic Sea. *Remote Sens Environ* 89:326–350
- Dekker AG (1993) Detection of optical water quality parameters of eutrophic waters by high resolution remote sensing. PhD thesis. Vrije Universiteit, Amsterdam, The Netherlands
- Forsberg BR, Devol AH, Richey JE, Martinelli Santos H (1988) Factors controlling nutrient concentrations in Amazon floodplain lakes. *Limnol Oceanogr* 33:41–56
- Forsberg BR, Araujo-Lima CARM, Martinelli LA, Victoria RL, Bonassi JA (1993) Autotrophic carbon sources for fish of the Central Amazon. *Ecology* 74:643–652
- Galvão LS, Pereira Filho W, Abdon MM, Novo EMM, Silva JSV, Ponzoni FJ (2003) Spectral reflectance characterization of shallow lakes from the Brazilian Pantanal wetland with field and airborne hyperspectral data. *Int J Remote Sens* 24:1–20
- Goodin DG, Han L, Fraser RN, Rundquist C, Stebbins WA, Schalles JF (1993) Analysis of suspended solids in water using remotely sensed high resolution derivative spectra. *Photogram Eng Remote Sens* 59:505–510
- Hess LL, Melack JM, Novo ELM, Barbosa CCF, Gastil M (2003) Dual-season mapping of wetland inundation and vegetation for the central Amazon basin. *Remote Sens Environ* 87:404–428
- Isaac JV, Oliveira C, Azevedo CR, Mello RQ (2003) Estudo das atividades pesqueiras no Lago Grande de Curuaí. Região do Médio Amazonas. Provarzea/IBAMA, Manaus
- Keiner LE, Yan XA (1998) Neural network model for estimating seasurface chlorophyll and sediments from Thematic Mapper imagery. *Remote Sens Environ* 66:153–165
- Kirk JTO (1994) Light and photosynthesis in aquatic ecosystems, 2nd edn. Cambridge University Press, Cambridge
- Koponen S, Kallio K, Pulliainen J, Vepsäläinen J, Pyhälähti T, Hallikainen M (2004) Water quality classification of lakes using 250-m MODIS data. *IEEE Geosci Remote Sens Lett* 1:287–291
- Kwiatkowska EJ, Fargion GS (2003) Application of machine-learning techniques toward the creation of a consistent and calibrated global chlorophyll concentration baseline dataset using remotely sensed ocean color data. *IEEE Trans Geosci Remote Sens* 41:2844–2860
- Lathrop RG, Lillesand TM (1986) Use of Thematic Mapper data to assess water quality in Green Bay and central Lake Michigan. *Photogram Eng Remote Sens* 52:671–680
- Lesack LFW, Melack JM (1995) Flooding hydrology and mixture dynamics of lake water derived from multiple sources in an Amazon floodplain lake. *Water Resour Res* 31:329–345
- Melack JM, Forsberg B (2001) Biogeochemistry of Amazon floodplain lakes and associated wetlands. In: McClain ME, Victoria RL, Richey JE (eds) *The biogeochemistry of the Amazon basin and its role in a changing world*. Oxford University Press, New York, pp 235–276
- Mertes LAK (1990) Hydrology, hydraulics, sediment transport and geomorphology of the central Amazon floodplain. PhD dissertation. University of Washington, Seattle
- Mertes LAK (1997) Documentation and significance of the perirheic zone on inundated floodplains. *Water Resour Res* 33:1749–1762
- Mertes LAK, Daniel DL, Melack JM, Nelson B, Martinelli A, Forsberg BR (1995) Spatial patterns of hydrology, geomorphology, and vegetation on the floodplain of the Amazon River in Brazil from a remote sensing perspective. *Geomorphology* 13:215–232
- Miller RL, McKee BA (2004) Using MODIS Terra 250m imagery to map concentrations of total suspended matter in coastal waters. *Remote Sens Environ* 93:259–266
- Mobley CD (1994) Light and water: radiative transfer in natural waters. Academic Press, San Diego
- Morel A, Berthon JF (1989) Surface pigments, algal biomass profiles, and potential production of the euphotic layer: relationships reinvestigated in view of remote-sensing applications. *Limnol Oceanogr* 34:1545–1562

- Morel A, Prieur L (1977) Analysis of variations in ocean color. *Limnol Oceanogr* 22:709–721
- Novo EMLM, Shimabukuro YE (1994) Spectral mixture analysis of inland tropical waters. *Int J Remote Sens* 15:1354–1356
- Novo EMLM, Steffen CA, Braga CZF (1991) Results of a laboratory experiment relating spectral reflectance to total suspended solids. *Remote Sens Environ* 36:67–72
- Nush EA (1980) Comparison of different methods for chlorophyll and phaeopigment determination. *Arch Hydrobiol* 4:14–36
- Pilorz SH, Davis CO (1990) Spectral decomposition of sea surface reflected radiance. *IGARSS 1990 Proc* 1:345–348
- Richey JE, Nobre C, Deser C (1989) Amazon River discharge and climate variability: 1903–1985. *Science* 246:101–103
- Richey JE, Wilhelm SR, McClain ME, Victoria RL, Melack JM, Araujo-Lima C (1997) Organic matter and nutrient dynamics in river corridors of the Amazon basin and their response to anthropogenic change. *Ciênc Cult (Sao Paulo)* 49:98–110
- Shimabukuro YE, Smith JA (1991) The least squares mixing models to generate fraction images derived from remote sensing multispectral data. *IEEE Trans Geosci Remote Sens* 29:16–20
- Sippel SJ, Hamilton SK, Melack JM (1992) Inundation area and morphology of lakes on the Amazon River floodplain, Brazil. *Arch Hydrobiol* 123:385–400
- Tassan S (1995) SeaWiFS potential for remote sensing of marine *Trichodesmium* at sub-bloom concentration. *Int J Remote Sens* 16:3619–3627
- Wetzel RG, Likens GE (1991) *Limnological analyses*, 2nd edn. Springer, New York